Droplet transport in a polymer-coated nanochannel

Kevin Speyer* and Claudio Pastorino*

*Departamento de Materia Condensada, Centro Atómico Constituyentes CNEA-CONICET, Buenos Aires, Argentina

pastor@cnea.gov.ar

Abstract

We study the influence of chain stiffness on droplet flow in a nano-channel, coated with semiflexible hydrophobic polymers by means of non-equilibrium molecular-dynamics simulations. The studied system is then a moving droplet in the slit channel, coexisting with its vapor and subjected to periodic boundary conditions in the flow direction. The polymer chains, grafted by the terminal bead to the confining walls, are described by a coarse-grained model that accounts for chain connectivity, excluded volume interactions and local chain stiffness. The rheological, frictional and dynamical properties of the brush are explored over a wide range of persistence lengths. We find a rich behavior of polymer conformations and concomitant changes in the friction properties over the wide range of studied polymer stiffnesses. A rapid decrease in the droplet velocity was observed as the rigidity of the chains is increased for polymers whose persistence length is smaller than their contour length. We find a strong relation between the internal dynamics of the brush and the droplet transport properties, which could be used to tailor flow properties by surface functionalization. The monomers of the brush layer, under the droplet, present a collective "treadmill belt" like dynamics which can only be present due the the existence of grafted chains. We describe its changes in spatial extension upon variations of polymer stiffness, with bidimensional velocity and density profiles. The deformation of the polymer brushes due to the presence of the droplet is analyzed in detail. Lastly, The droplet-gas interaction is studied by varying the liquid to gas ratio, observing a 16% speed increase for droplets that flow close to each other, compared to a train of droplets that present a large gap between consecutive droplets.

Introduction

System of Interest

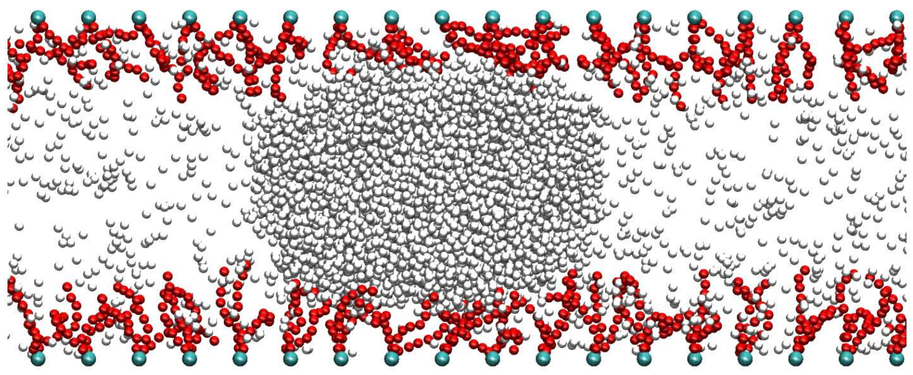

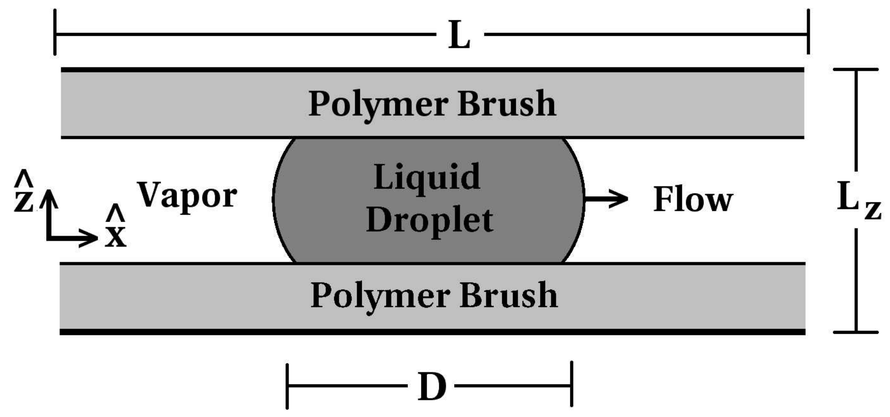

Snapshot of the simulated nano-channel. The semiflexible polymer chains (in **red**) are grafted by the end bead (in **light blue**) to the wall of the channel. The fluid (droplet + vapor) inside the channel is composed by particles (in **gray**) interacting via a Lennard-Jones potential. Periodic boundary conditions are imposed in directions $\hat{x}$ and $\hat{y}$. An external constant force is applied to all particles in $\hat{x}$ direction.

Model and Simulation Techniques

- Molecular Description: Coarse grain, bead spring model.
- **Molecular Dynamics (MD) + Dissipative Particle Dynamics Thermostat (DPD)**

Interactions

- **Chain Connectivity** between contiguous *beads* of the same polymer. Finitely extensible non-linear elastic potential(FENE):

$$U_{\text{FENE}} = \begin{cases} -\frac{1}{2}k\ R_0^2 \ln\left[1-(\frac{r}{R_0})^2\right] & r \le R_0 \\ \infty & r > R_0 \end{cases}, \qquad \text{where } R_0 = 1.5\sigma,\ k = 30\varepsilon/\sigma^2 \text{ and } r = |\mathbf{r}_i - \mathbf{r}j| \ .$$

- **Monomer-Monomer Potential**

$$U(r) = \begin{cases} 4\varepsilon[(\frac{\sigma}{r})^{12} - (\frac{\sigma}{r})^6 - U_{LJ}(r_c)] & r \le r_c \\ 0 & r > r_c \end{cases},$$

Hidrophobic liquid-brush interaction

$$\varepsilon^{liq-cep} = \frac{1}{3}\varepsilon^{liq-liq} = \frac{1}{3}\varepsilon^{cep-cep}$$

$\sigma = 1$. Polymer cut radius: $r_c = 2^{\frac{1}{6}}$ (polymers in good solvent conditions).

- **Wall-Monomer Potential**

$U_{\text{wall}}(z) = |A_w|(\frac{\sigma_w}{z})^9 - A_w(\frac{\sigma_w}{z})^3$, with $A = -3.2\varepsilon$. The walls, fixed at $z = 0$ and $z = D$, are impenetrable and have no intrinsic roughness.

- **Bending Potential**

$$U_{\text{bend}}(\theta) = \frac{1}{2}k_{\text{b}}\theta^2$$

This potential favours chain stretching and adds rigidity to the polymer. A wide range of bending constants (k_{b}) were implemented to explore the different rigidity regimes: $0 < k_{\text{b}} < 160\varepsilon$
Or in terms of persistence length (l_p) over contour length (l_c): $0 < l_p/l_c < 22$
The reduced persistence length (l_p/l_c) is the dimensionless quantity that meassures the polymer rigidity.

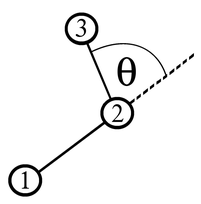

Results

Polymer Dynamics

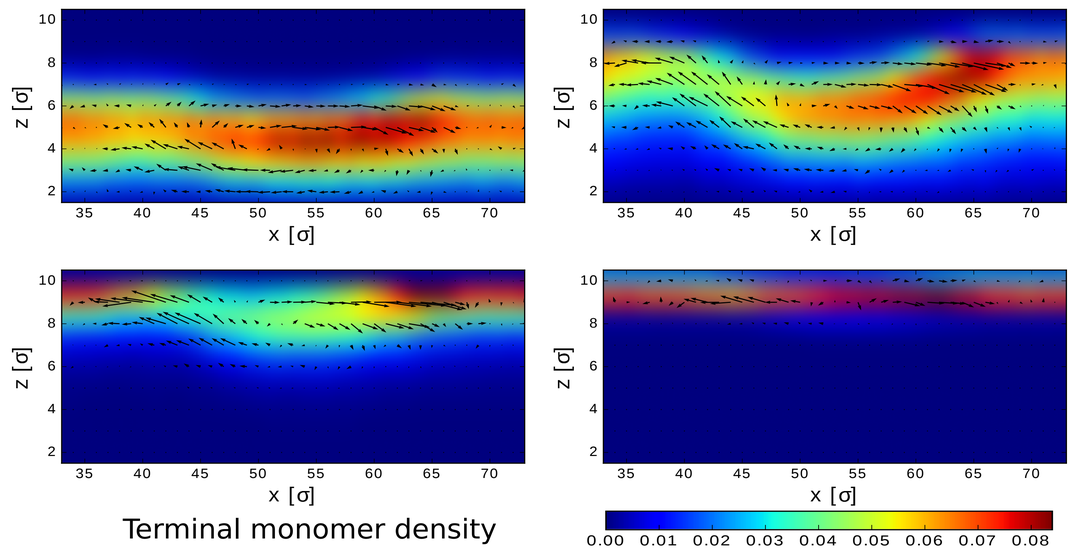

Polymer's end-bead distribution is shown as a color map. The correspondence between colors and monomer density (given in units of σ^{-3}) is shown in the color bar at the bottom. The black arrows, composing a vector field, represent the mean momentum of the end-beads of the polymers. These graphs are presented for various rigidities, from left to right and top to bottom: $l_p/l_c = 0.1;\ 0.72;\ 2.9;\ 8.3$.

Droplet Velocity vs Polymer Rigidity

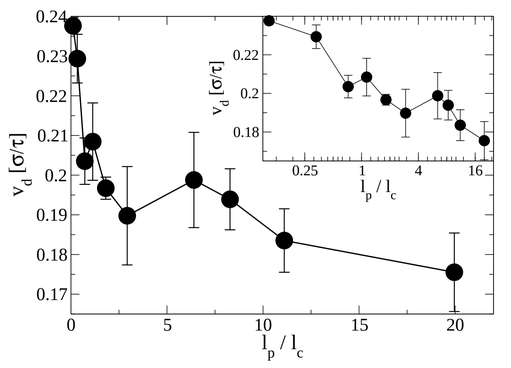

Droplet velocity with respect to the reduced persistence length of the polymers. The inset shows the droplet velocity plotted against the persistence length in a semi-log graph to highlight the behavior at low persistence lengths. For $l_p/l_c < 2$ the droplet velocity decreases rapidly with increasing polymer rigidity. The liquid velocity is highly influenced by the polymer dynamics.

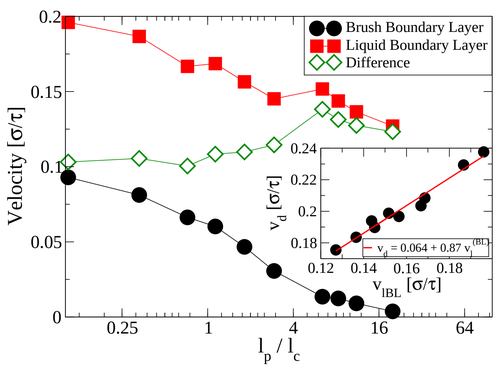

Velocity of the brush (black circles) and liquid (red squares) in the brush-liquid interface are plotted with respect to the reduced persistence length. The difference between these velocities, shows how the liquid boundary layer passes over the brush boundary layer (open green diamonds). Inset: droplet velocity versus the liquid boundary layer velocity.

Flow Across the Channel

Fluid velocity in the direction of the flow ($\hat{x}$) as a function of the x coordinate (in log scale). The droplet ($x < 48\sigma$) travels at a higher velocity than the vapor phase ($x > 48\sigma$). It is also possible to observe that gas velocity decays exponentially with x. Inset: 2-dimensional density profile of the droplet, with the liquid velocity field overlayed. The velocities are calculated in the frame of reference of the center of mass of the droplet. The color legend shows the liquid number density in units of σ^{-3}.

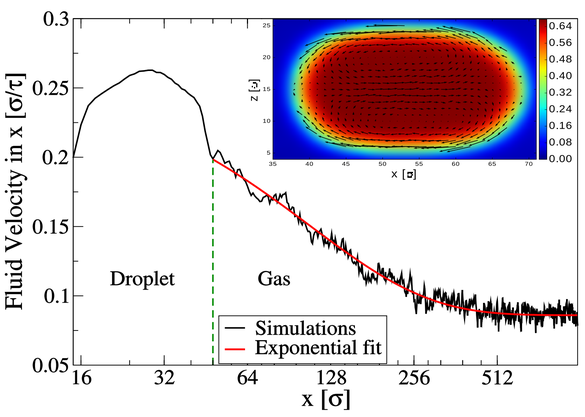

References

K. Speyer and C. Pastorino, *Soft Matter*, 2015, DOI: 10.1039/C5SM01075F
K. Speyer and C. Pastorino, *Langmuir*, 2017, DOI: 10.1021/acs.langmuir.7b02640